Remote sensing and GIS technology in the Global Land Ice Measurements from Space (GLIMS) Project

Bruce Raup[a],*, Andreas Kääb[b], Jeffrey S. Kargel[c], Michael P. Bishop[d], Gordon Hamilton[e], Ella Lee[f], Frank Paul[b], Frank Rau[g], Deborah Soltesz[f], Siri Jodha Singh Khalsa[a], Matthew Beedle[a], Christopher Helm[a]

[a]National Snow and Ice Data Center, University of Colorado, 449 UCB, Boulder, CO 80309, USA
[b]Glaciology and Geomorphodynamics Group, Department of Geography, University of Zurich, Winterthurerstr. 190, CH-8057 Zurich, Switzerland
[c]University of Arizona, 1133 E. North Campus Dr., Tucson, AZ 85721, USA
[d]Durham Science Center, University of Nebraska at Omaha, 267 Omaha, NE 68182-0199, USA
[e]Climate Change Institute, University of Maine, Maine, USA
[f]US Geological Survey, 2255 N. Gemini Dr., Flagstaff, AZ 86001, USA
[g]Inst. Physische Geographie, University of Freiburg, Werderring 4, D-79085 Freiburg, Germany

Abstract

Global Land Ice Measurements from Space (GLIMS) is an international consortium established to acquire satellite images of the world's glaciers, analyze them for glacier extent and changes, and to assess these change data in terms of forcings. The consortium is organized into a system of Regional Centers, each of which is responsible for glaciers in their region of expertise. Specialized needs for mapping glaciers in a distributed analysis environment require considerable work developing software tools: terrain classification emphasizing snow, ice, water, and admixtures of ice with rock debris; change detection and analysis; visualization of images and derived data; interpretation and archival of derived data; and analysis to ensure consistency of results from different Regional Centers. A global glacier database has been designed and implemented at the National Snow and Ice Data Center (Boulder, CO); parameters have been expanded from those of the World Glacier Inventory (WGI), and the database has been structured to be compatible with (and to incorporate) WGI data. The project as a whole was originated, and has been coordinated by, the US Geological Survey (Flagstaff, AZ), which has also led the development of an interactive tool for automated analysis and manual editing of glacier images and derived data (GLIMSView). This article addresses remote sensing and Geographic Information Science techniques developed within the framework of GLIMS in order to fulfill the goals of this distributed project. Sample applications illustrating the developed techniques are also shown.

*Corresponding author. Tel.: +1 303 492 8814.
E-mail address: braup@nsidc.org (B. Raup).

1. Introduction

Glaciers, ice caps, and ice sheets are important components of Earth's natural systems and of human environments, and are therefore obvious targets for mapping and monitoring. They moderate extremes in hydrological cycles, important to people living in arid regions (Yang and Hu, 1992). Melting ice bodies contribute to the rise in global sea level (Gregory and Oerlemans, 1998; Church et al., 2001). They are natural integrators of changes in climate, and serve as sensitive indicators of climate change (Haeberli and Beniston, 1998). The climate change linkage is so strong that many small glaciers that existed a few decades ago are now gone, and many existing today will probably disappear within a few more years or decades (Dyurgerov and Meier, 2000; Haeberli and Beniston, 1998; Hastenrath and Geischar, 1997; Paul et al., 2004b). The linkage has been examined both ways, with some studies considering climatic change inputs and calculating glacier responses, and other studies measuring glacier changes and back-calculating global warming (Oerlemans, 2005). Glaciers can also pose significant hazards to people (Kääb et al., 2002). The mass balance of a glacier (net mass change over the course of one year, usually measured at the end of the melt season) responds immediately to changes in annual meteorological conditions, whereas glacier areal extent and length respond after a delay related to the dynamics of the glacier motion (Paterson, 1994). Field methods provide the best means to obtain detailed, uncompromised, and reliable information on glacier mass balance and some other critical measurements. While airborne remote sensing provides critical information on ice sheet profiles, thickness, melt patterns, and flow fields, satellite remote sensing is the only means by which to acquire comprehensive, uniform, and frequent global observations of glaciers and ice sheets. This is simply because glaciers are numerous (approximately 2×10^5), and they and the two ice sheets (Greenland and Antarctica) are widespread and generally remote from research institutions and population centers.

Many remote sensing methods have been developed for land ice. The best-established techniques for mapping and monitoring ice extent use the optical part of the electromagnetic spectrum. Multi-spectral imaging in the visible and infrared is unsurpassed for certain types of terrain classification and other requirements for systematic global study of glaciers (e.g., Albert, 2002; Paul et al., 2002; Williams and Ferrigno, 2002). Some of the most promising methods developed recently include satellite radar interferometry and radar speckle tracking for measuring flow displacement fields (Bamber et al., 2000; Joughin, 2002; Rignot et al., 2004a; Strozzi et al., 2002), passive microwave measurements of temperature and melt zones (Abdalati and Steffen, 2001), and laser altimetry and laser scanning for measuring glacier and ice sheet surface topography and their changes over time (Baltsavias et al., 2001; Geist and Stötter, 2003; Krabill et al., 2004). Several remote sensing methods applied to glaciers, ice caps, and ice sheets have indicated that these bodies sometimes show surprisingly fast dynamical responses to environmental changes, rapidly evolving effects of melt water, unpinning due to breakup of ice shelves, and other instabilities (Abdalati and Steffen, 2001; Abdalati et al., 2001, 2004; Joughin et al., 2002; Krabill et al., 1999; Paul et al., 2004b; Rignot et al., 2004a, b; Zwally et al., 2002). Many of the above data types are complementary to each other. Methods for relating field-observable quantities (e.g., mass balance) to space-based observables (glacier length or area) have been developed (Dyurgerov and Bahr, 1999).

This article discusses technology hurdles and developments relevant to completion of the goals of the Global Land Ice Measurements from Space (GLIMS) project. The ambitious scope, complex analysis tasks, and the necessary international consortium approach require considerable technology development both to enable the required types of analysis and to ensure reliability, coherence, and accessibility of the derived data. We first describe areas of technology development for GLIMS and then present some representative GLIMS glacier science and practical applications.

2. GLIMS

The GLIMS project was established to acquire satellite multi-spectral images of the world's glaciers and analyze them for glacier extent and changes, and to understand these change data in terms of climatic and other forcings (Kieffer et al., 2000; http://www.glims.org/). GLIMS was initiated and originally coordinated by the US Geological Survey

(Flagstaff, AZ). The scope of the goals of GLIMS requires an international consortium, which currently involves researchers from 27 countries. GLIMS is organized into a system of Regional Centers, which were originally intended to be established on geographical terms; for practical reasons (due to involvement of national funding agencies) GLIMS Regional Centers, with few exceptions, instead have been based on political boundaries. The Regional Centers include a network of collaborating stewards, who may be responsible, for instance, for analysis of a single glacier or may take on broader roles. As of March 2006, there are currently 71 registered Regional Centers, Stewards, and core institutions, involving approximately 110 people. Glacier data produced at Regional Centers are ingested into the GLIMS Glacier Database, designed and constructed at the US National Snow and Ice Data Center (NSIDC), in Boulder, CO. This database is described in detail in Section 4.

Other groups have formed with the purpose of building databases of glacier data. The World Glacier Monitoring Service (WGMS) was established in 1986 in order to continue building a glacier inventory begun in 1894, which consists of point locations, area, elevation range, classification, and many other parameters. The inventory, called the World Glacier Inventory (WGI), contains approximately 70 000 glaciers. Although this inventory is occasionally updated, it is essentially a static snapshot of glaciers, and not designed to enable tracking of glacier evolution over time. The WGI is currently the most comprehensive inventory of world glaciers, and the WGMS continues to publish volumes on glacier fluctuations. The GLIMS database has been designed to be a logical extension to the WGI. Another project, Omega, aimed to study the glaciers of Europe in a multi-pronged manner using a variety of ground-based methods as well as remote sensing. The project has been completed, and we are discussing with Omega researchers how their data can be incorporated into the GLIMS Glacier Database.

The primary product of GLIMS is the GLIMS Glacier Database, the first global glacier database to include complete glacier outlines. While some analysis, such as summary statistics, will be done on the data within GLIMS, we expect the database to be used as input to many more separately funded investigations into links between the world's glaciers and other Earth systems.

2.1. Data

GLIMS originated as an Advanced Spaceborne Thermal Emission and Reflection Radiometer (ASTER) Science Team effort, and ASTER imagery is ideal in many regards to fulfill the goals of GLIMS, although other image data, such as Landsat Enhanced Thematic Mapper Plus (ETM+), older Landsat, and synthetic aperture RADAR (SAR) imaging and historic maps and air photos, help to fill gaps, extend coverage over several decades, and provide important complementary observations. GLIMS is an ASTER Science Team activity, and we have submitted ASTER image acquisition requests to the ASTER Ground Data System for (nominally) annual acquisitions of imagery over all glaciers, ice caps, and ice sheet margins on Earth, with requested imaging season and instrument gain settings optimized for glaciers (Raup et al., 2000). Although the primary data source for GLIMS is currently focused on optical imagery, glacier boundaries and other glaciological data derived from other sources, such as SAR imagery or older maps may also be incorporated into the GLIMS Glacier Database. For example, we have ingested the Chinese Glacier Inventory data, which were derived from maps made in the mid-20th Century.

GLIMS is using imagery primarily from ASTER and Landsat 7 ETM+. Landsat 7 covers approximately 10 times the area per scene, while ASTER has finer spectral resolution in the short-wave infrared. Fig. 1 summarizes the spectral coverage of the ASTER and Landsat instruments. Additionally, ASTER carries a 15 m resolution near-infrared band looking $27.6°$ backwards from nadir. This band 3B covers the same spectral range of $0.76–0.86 \, \mu m$ as the nadir-looking band 3N, thus providing along-track stereo imaging. The look direction for band 3B is close to northward for low- to mid-latitudes. Along-track stereo is preferable to cross-track stereo for most applications in glaciology, since the two images are obtained during one overflight without marked terrain changes (both images of the stereo pair are acquired within about 1 min). During the longer time spans between the pairs of cross-track stereo imagery (up to months), the terrain conditions could change significantly, especially in mountain regions, and complicate image correlation, for instance, due to changes in snow pack. Within GLIMS, ASTER along-track stereo data are employed to generate Digital
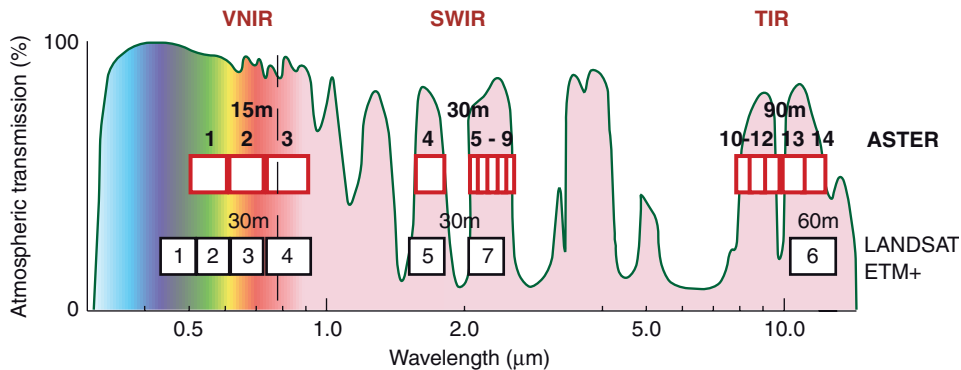
Fig. 1. Spectral bands of ASTER and Landsat ETM + satellite instruments (red and black boxes, respectively), together with atmospheric transmission (black curve) and typical snow reflectance (blue curve).

Elevation Models (DEMs) photogrammetrically. These DEMs have a horizontal resolution of about 30 m and a vertical resolution of about 20 m. For comparative studies, we have also used topographic data from the Shuttle Radar Topography Mission (SRTM). This near-global DEM has spatial resolutions of 30 m and 90 m, and was generated from data acquired during February 2000. Spatial coverage is between 56°S and 60°N latitudes.

Although only cloud-free imagery from the end of the ablation period can be used for efficient glacier mapping, appropriate scenes from nearly all glaciers over the world are available today, due to the long time period covered (starting with Landsat Thematic Mapper (TM) in 1982). However, the high cost of pre-Landsat-7 data has prevented their global application. With the launch of the Terra satellite and its sensor ASTER as well as the Landsat 7 Enhanced Thematic Mapper Plus (ETM +) in 1999, global glacier monitoring becomes achievable and is now being carried out by GLIMS and similar projects. The costs of ASTER data are waived for NASA principal investigators, and the use of ETM + data is made less expensive through the existence of data pools, including the Global Land Cover Facility.

Both ETM + and ASTER are multi-spectral instruments that have bands in the visible, near-infrared, and thermal infrared parts of the spectrum. ASTER's bands are divided into three subsystems: visible and near infrared (VNIR), short-wave infrared (SWIR), and thermal infrared (TIR). ASTER's five thermal bands are processed into three standard data products, available from EROS Data Center (EDC, South Dakota) as kinetic

temperature (AST08), radiant (brightness) temperature (AST04), and surface emissivity (AST05).

3. Methods

A distributed and large-scale project such as GLIMS presents unique challenges. Because of the large number of glaciers, image analysis and classification must be automated to a large degree, but glaciers vary tremendously from region to region. Reflectance properties of glacier surfaces are highly varied due to temporally and spatially variable patterns of dry snow, wet snow, recrystallized snow, and firn; clear water and turbid water; blue glacier ice, bubbly gray ice, and ice containing embedded fine debris; and ice partially or entirely covered by rock debris (both dry and wet debris). Stagnant debris-rich ice can even support sparse vegetation or even mature forests. Debris-covered glaciers require extensions to standard multi-spectral algorithms for boundary delineation. These methods usually involve a DEM, so we must be able to generate DEMs in snow-covered areas of high relief. DEMs also yield important glacier parameters such as minimum, maximum, and mean elevations, hypsography (Paul et al., 2002; Kääb et al., 2002), and even changes in thickness and volume. All analysts must use the same data model for representing glacier parameters to ensure error-free transmission of analysis results to the central database. The database must be designed to accommodate data on many types of glaciers including mountain glaciers, ice caps, outlet glaciers attached to large ice sheets, ice bodies that are disintegrating and detaching from each other, and glaciers that are connected to each other but have

different names and, for historic reasons, are treated separately. Special attention must be paid to consistency in the assembled global database, due to the fact that different algorithms are necessary for different regions. Finally, an interface to the database must enable end users to explore the multiple dimensions of the dataset.

GLIMS technology developments have encompassed many areas and have resulted in a growing and already robust capability for glacier analysis using satellite imagery, and for archival and manipulation of derived measurements and other value-added data. The following sections discuss a glacier digitization software tool built within the GLIMS project (GLIMSView), several glacier classification algorithms, the use and generation of DEMs, the design and structure of the GLIMS Glacier Database, and steps taken to ensure consistent results from our many Regional Centers. These algorithms, processing protocols, and the GLIMS glacier model are described in several technical documents available on the GLIMS website http://www.glims.org/.

3.1. GLIMSView

A key component of the GLIMS project is the creation of software tools to assist the extraction of glacier information from imagery in a consistent way across Regional Centers, and to package that information with appropriate metadata for transfer to NSIDC for insertion into the GLIMS Glacier Database. GLIMS Regional Centers use a wide variety of computer operating systems and image analysis tools, and have varying levels of glaciological, remote sensing, and computer expertise. Furthermore, varying funding levels across Regional Centers mean that many of them cannot afford expensive commercial software packages. GLIMS-View is a cross-platform application intended to aid and standardize the process of glacier digitization for the GLIMS project. Specifically, it allows the users to view various types of satellite imagery, digitize glacier outlines within the images and identify other material units of interest (or read such layers in from other digitization tools, such as commercial GIS software), attach GLIMS-specific attributes to segments of these outlines, and save the outlines and associated attribute data to a specially designed data transfer format (based on ESRI shapefiles) for ingest into the GLIMS Glacier Database. It focuses on the glacier boundary

digitization task, and leaves most image pre-processing steps to other software.

GLIMSView contains the core functionality needed by the GLIMS project. It supports imagery files in many formats, as well as ESRI shapefiles. GLIMSView provides a suite of tools for (1) digitizing glacier outlines and classifying other terrain features within and around the glaciers; (2) collecting metadata about the glaciers, the analysis session, and the analyst; and (3) assisting the analyst in providing complete and consistent information for database ingest. The latter is assured by presenting the analyst a consistent interface to the mandatory metadata fields. GLIMSView provides tools for image enhancement, and simple material classification by band arithmetic and thresholding. For production of vector outlines of glaciers, manual digitization of glacier boundaries is currently the primary method supported, but other methods are under active development. GLIMS-View uses a plug-in architecture so that new algorithms, implemented in C++, can be added easily. The application supports the creation and management of GLIMS glacier IDs. All digitized outlines, glacier IDs, and metadata can be exported into the GLIMS Data Transfer Format, a hierarchical set of ESRI shapefiles designed for the transfer of GLIMS data. A typical window in GLIMSView is shown in Fig. 2. In the near future, the application will support more sophisticated classification algorithms, including those using DEMs as input. GLIMSView is built on top of several popular Open Source libraries, including Qt (http://www.trolltech.com), the Geospatial Data Abstraction Library (GDAL, http://www.remotesensing.org/gdal/), the HDF and HDF-EOS libraries (http://newsroom.gsfc.nasa.gov/sdptoolkit/toolkit.html), and Proj.4 Cartographic Projections Library (http://proj.maptools.org/). GLIMSView is freely available to all, and is distributed in both compiled and source forms on the GLIMS website (http://www.glims.org/software/). GLIMSView runs on Linux and Windows, and will soon run on Mac OS X.

3.2. GLIMS technology developments

The term *image classification* usually refers to the process of associating *material* labels (e.g., vegetation, snow) with pixels in an image. Ultimately, GLIMS requires vector outlines delineating glacier boundaries. The process of creating glacier bound-
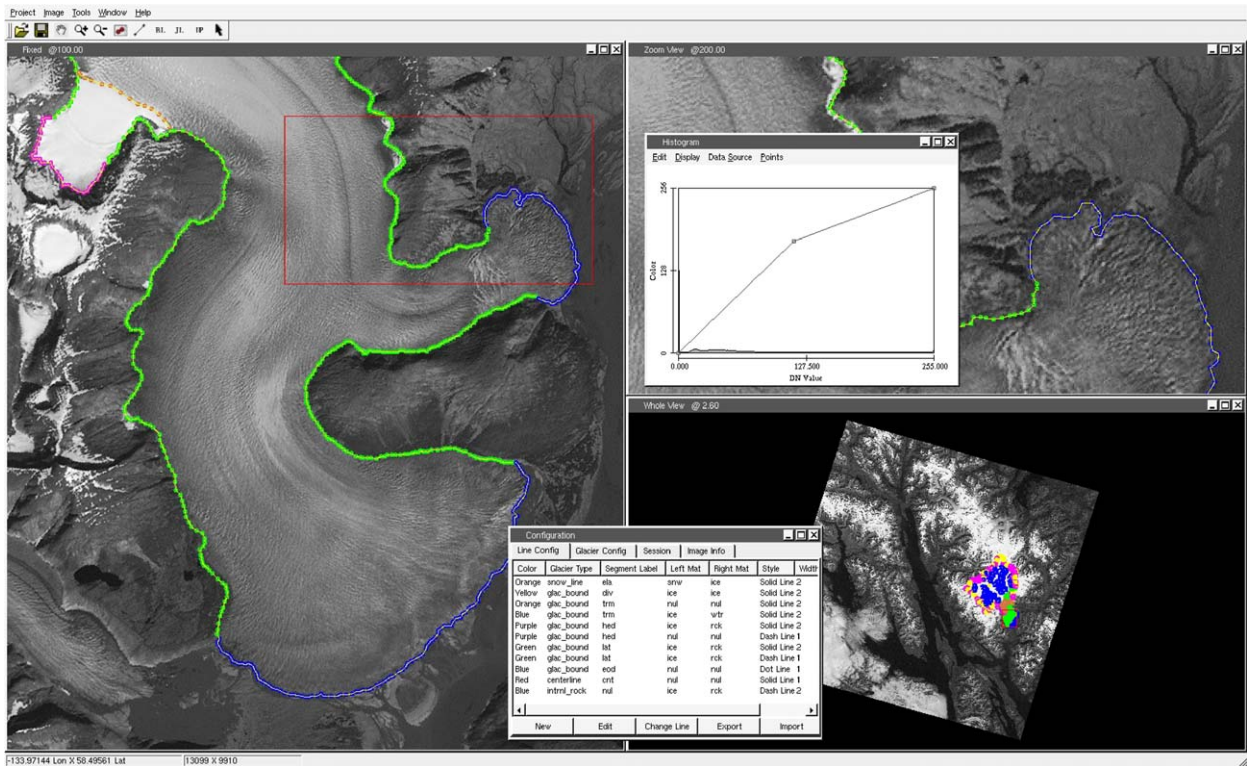
Fig. 2. Outlines for Taku Glacier, Alaska (59.3°N, 134°W), shown in a session using GLIMSView software. Outlines were manually digitized by an operator familiar with region, from field observations. Some of GLIMSView's more important dialogs are also shown.

Table 1
Summary of glacier outline extraction methods

Classification Method	Suitable terrain type
Manual digitization	Any
Spectral band ratio and threshold	Clean glacier ice and snow
Normalized Difference Snow Index	Clean glacier ice and snow
Geomorphometric-based methods	Debris-covered glaciers
Thermal band methods	Clean or lightly debris-covered glaciers

aries automatically from an image typically begins with classification of the materials within the image. After that, the analyst must use a combination of (1) assumptions about what materials compose glaciers and (2) additional information about topography, texture, or other geomorphometric parameters to identify which pixels are *glacier* pixels. A glacier can manifest a variety of material types on its surface. These glacier regions are then circumscribed by vector outlines. This process can be done directly via manual digitization, or using algorithms described below.

The algorithms required to effectively extract glacier outlines from satellite images containing different types of landscape frequently require tailoring the algorithm to each region, since different glaciers may contain various admixtures of ice, snow, rock debris, and even vegetation. There is no one algorithm that is suitable to all regions. Table 1 summarizes the main algorithms being used by the GLIMS Regional Centers. In the sections that follow, we present results from each method and discuss some of the technical details behind them.

3.2.1. Manual digitization

Human interpretation remains the best tool for extracting higher level information from satellite imagery for many glacier types. Tedious, manual digitization of glacier boundaries by an operator knowledgeable of the region can produce glacier boundary outlines of high quality and accuracy. Examples of manual classification in the GLIMS Glacier Database include the outlines of several glaciers in Alaska. Fig. 2 shows outlines for the large Taku Glacier (near Juneau, 59.3°N, 134°W), which were digitized manually by Matthew Beedle at the University of Colorado using GLIMSView. The delineation of flow divides (ice–ice boundaries between glaciers flowing in locally opposite directions) is more difficult, but can be aided by using a DEM.

3.2.2. Multi-spectral classification methods

Nearly 20 years of glacier mapping from Landsat TM data has resulted in an abundance of methods. From the numerous automatic snow-and-ice mapping methods available, one category of classifiers consistently provides accurate glacier classification results for the non-specialist in image processing: simple band math (using only $+$, $-$, $*$, $/$) based on the distinct low reflectance of ice and snow in the short-wave infrared part of the spectrum and its high reflectance in the visible part (e.g., Bayr et al., 1994; Kääb et al., 2003; Paul, 2002; Paul et al., 2002). As this spectral region is covered by several spaceborne sensors (e.g., ASTER, IRS-1C/ D, Landsat TM/ETM +, SPOT 4/5), the method is widely applicable. The latest reviews and comparisons (of these and other methods) are given by Sidjak and Wheate (1999); Gao and Liu (2001); Albert (2002); Paul et al. (2002); Paul (2004) and Bishop et al. (2004).

Glacier classification methods based on thresholded simple band ratios (e.g., ASTER3/ASTER4) or normalized band differences like the NDSI (e.g., (TM2−TM5)/(TM2+TM5)) have proven to be accurate, fast and robust methods for detection of clean glacier ice (Albert, 2002; Paul et al., 2002, 2003), though they can lead to errors where debris covers the ice. The glacier area obtained by applying a threshold to the ratio image is highly sensitive to the value of the threshold in regions with a low signal-to-noise ratio, such as those with snow and ice in cast shadow. In order to account for this sensitivity and to minimize the manual corrections afterwards, the final threshold for glacier mapping should be tested and selected in these cast shadow regions. An additional threshold
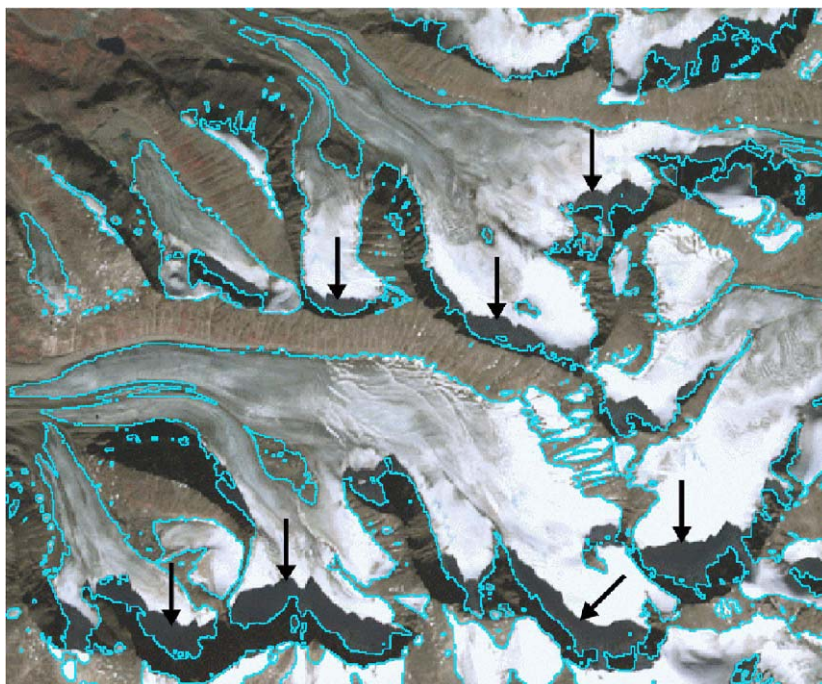

Fig. 3. Overlay of glacier outlines obtained from an AST3/AST4 ratio image including an additional threshold in AST1 with original band 3, 2, 1 composite. Glacier regions in cast shadow (arrows) are exactly captured. Image size is 10 km × 8.3 km; north is up.

in a visible band has been proven to efficiently eliminate misclassification in cast shadow when a TM3/TM5 or ASTER2/ASTER4 ratio is used, as depicted in Fig. 3 (Paul and Kääb, in press.). Due to a variation of illumination with latitude and time of the year (solar elevation), some time should be spent on finding the optimal band combinations and thresholds on a case-by-case basis. Within the GLIMS project, this type of algorithm refinement is done by the Regional Centers in coordination with the Algorithms Working Group.

Further sources of error in glacier classification can be reduced by application of image processing techniques: Vegetation can be classified beforehand from the Normalized Difference Vegetation Index (NDVI) to reduce misclassification when TM4/TM5 (ASTER4/ASTER4) ratios are applied; errors due to small snow patches and gaps due to debris cover can be reduced using a median filter, minimum area filters, or erode/dilate operations; one of the thermal bands can be used instead of the short-wave infrared band to allow classification of glacier ice under thin volcanic ash layers (e.g., on Vatnajøkull); and turbid water bodies can be detected from a ratio index such as the NDVI (Huggel et al., 2002), or detached from the glacier in the course of the basin delineation (Paul and Kääb, in press).

For most glacier classification purposes using ASTER, it is helpful or necessary to use SWIR bands, but for mapping fine-scale features (such as small supraglacial ponds, fine-scale medial moraines, and details of glacier margins), it is more useful to work solely with VNIR so as to take full advantage of the 15 m resolution of VNIR vs. 30 m for SWIR. A simple classifier using ASTER bands 1 and 3 was developed (B3R1/3, for Band 3 vs. Ratio Band1/Band 3), which is highly effective in isolating glacier lakes and giving a measure of their turbidity (cf. Huggel et al., 2002; Wessels et al., 2002). The algorithm was tested in three regions (Peru, Alaska, and Afghanistan) to make the algorithm more robust against image saturation over snow and ice, and shadowing.

B3R1/3 uses a supervised classification scheme (decision surfaces) based on cluster identification of units, which was fully manual in the examples given in this section but could use an automated cluster algorithm. Since the material units' spectral properties are defined empirically, these properties may be adapted from one image to another based on the particular circumstances and analysis needs. An example of a B3R1/3 output applied to a radiance-calibrated ASTER (AST07) image of Peru is given in Kargel et al. (2005).

The B3R1/3 classifier is useful primarily for identifying and characterizing proglacial glacier-fed lakes and isolated clear-water lakes, and this algorithm can be used to identify such water bodies at the 15 m resolution before using other multi-spectral methods to classify glacier ice, as described above.

It is planned that the above multi-spectral classification algorithms will be built into GLIMS-View soon.

3.2.3. Geomorphometry-based methods

Clean-ice glaciers and most glacier lakes are easily classified using VNIR data, and for more difficult or more complex classifications, addition of SWIR provides a variety of powerful material classifiers. However, the delineation of debris-covered glaciers is difficult, and remains the main bottleneck for rapid and automated assessment of glacier areas from satellite data. In many mountain environments that exhibit heavily debris-covered glaciers, such as Alaska, the Andes, and the Himalaya, traditional statistical–multi-spectral classification algorithms are of limited value because of the inherent difficulties in using pure multi-spectral data to separate, e.g., dirty, shadowed ice from extremely turbid water, or to separate debris-covered glacier ice from fresh, ice-free moraines. A number of methods have been proposed in the recent literature to address this problem. They use the additional information provided by topography (Bishop et al., 2001; Kieffer et al., 2000; Bishop et al., 2004), neighborhood analysis (Paul et al., 2004a) and thermal radiation (Taschner and Ranzi, 2002) for mapping debris-covered glaciers.

One approach that works well in complex topography incorporates object-oriented analysis and neural networks. The multi-stage processing sequence involves (1) classification of land cover using spectral data and topography; (2) spatial analysis of imagery to generate geometric, shape, and topological information; (3) geomorphometric analysis and spatial analysis of DEMs to generate unique topographic information; (4) fusion of data in an object-oriented parameterization scheme; and (5) classification of supraglacial features and glaciers via neural networks. Essentially, this approach characterizes the three-dimensional spatial variation of the landscape and permits constraints to be applied in the identification and classification of

debris-covered alpine glaciers. It offers the advantage of being a hybrid approach (i.e., human and computer-assisted analysis), although it significantly reduces error compared to traditional approaches and increases the consistency of results.

Simple examples demonstrate this capability, and we have developed software tools to facilitate semi-automated analysis. For processing stage 1, we train a simple three-layer neural network using the back-propagation learning algorithm (Rumelhart and McClelland, 1986). The use of neural networks addresses numerous problems in generating accurate classification results in mountain environments (Bishop et al., 2001). Samples are selected using a graphical user interface that permits an analyst to quickly extract training sample points or areas from any selected area within an ASTER scene. The decision of where to sample is facilitated by image and dynamic spectral curve display using simple key strokes and movement of the mouse. After sampling one area, the user can select another area within the scene. In this way, an analyst can quickly and effectively sample training data and produce neural network classification results (Fig. 4). This capability is important for GLIMS Regional Centers as they must inventory large areas and process large numbers of ASTER scenes. Fig. 4 also highlights some difficulties faced by all classification tools tested thus far across the GLIMS consortium; some areas of glacier lakes are classified along with dirty ice near the margins of the glacier. As with the output obtained by application of other tools, this
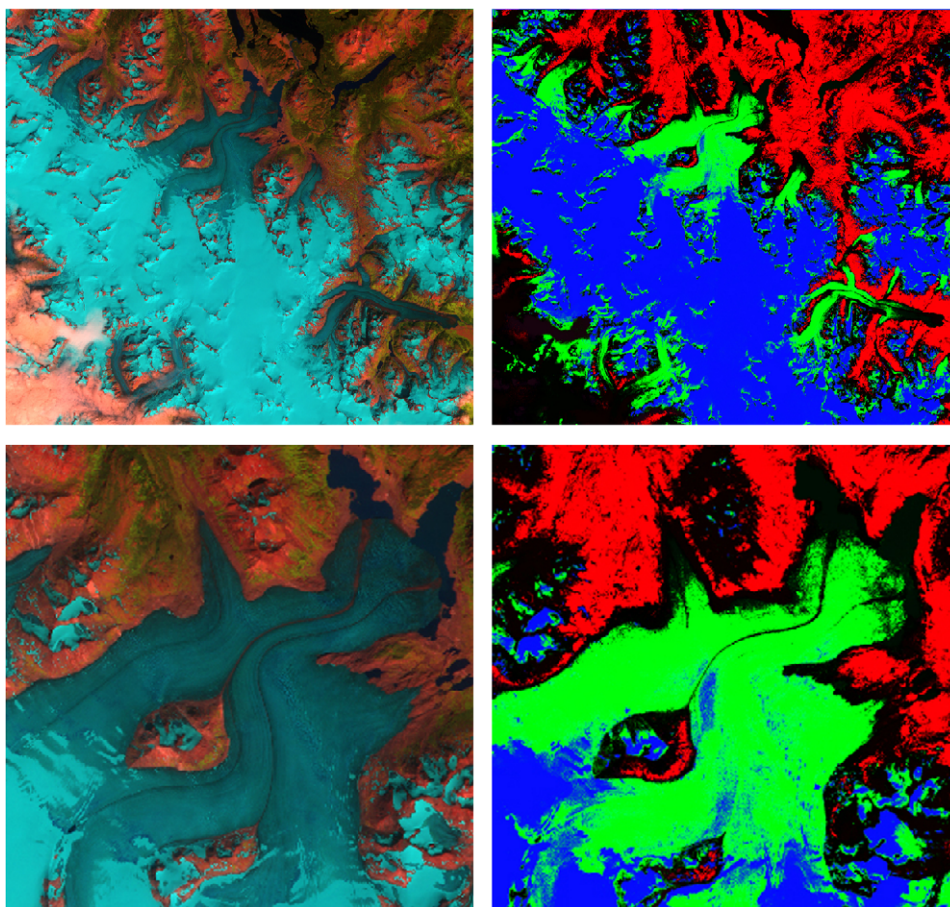

Fig. 4. An ASTER false-color composite (bands 4, 3, and 2) of Llewellyn Glacier, near Juneau, Alaska, USA (left). Neural network classification results using original spectral data (right) are in form of a false-color composite of fuzzy uncertainties. In general, blue is snow, green is ice, red is bare land or vegetation, and black is water or moisture-laden debris. Notice the ability of classification results to depict variation in glacier characteristics, such as debris cover and moisture-laden debris. These results were generated with minimal effort and training of a three-layer neural network for example purposes. Issues such as topographic variation and class differentiation tailored to a specific purpose can be easily addressed using spectral features and topographic information.
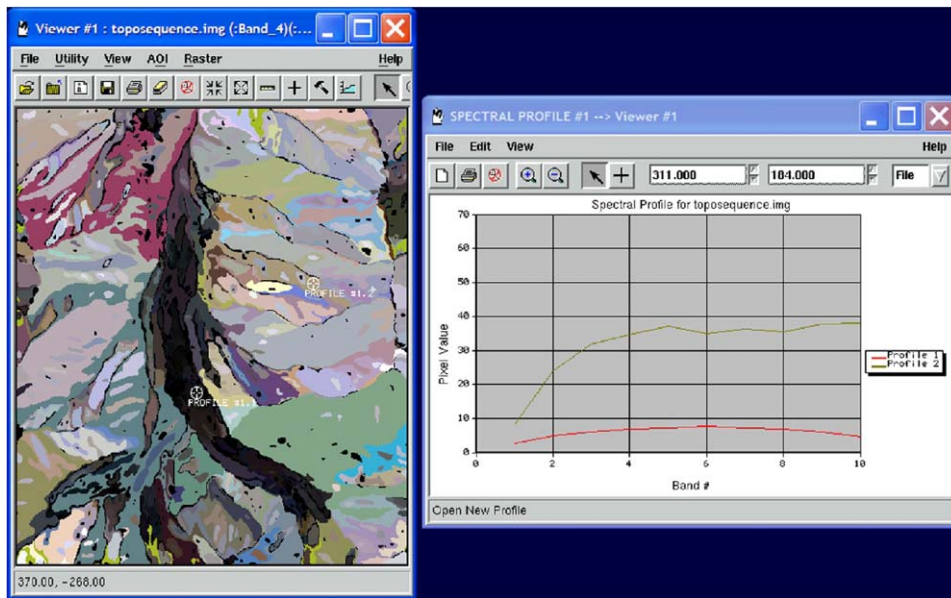
Fig. 5. Topo-sequence information in the form of variation in slope angle with altitude for Raikot Basin at Nanga Parbat, Pakistan. A slope-aspect image was generated and classified into eight homogeneous classes. Spatial clumping was used to identify individual objects, which then served as a basis for further geomorphometric analysis, such that each object has a unique topo-sequence curve. Displayed curves depict difference in this property of topography between a glacial surface and basin hill slopes.

mis-classification can be dealt with by human intervention and editing of the analysis results. The general need for iterative approaches to glacier delineation points out the basis for developing a highly interactive environment used in GLIMS-View.

An example illustrating the output of processing stage 3 is shown in Fig. 5. Topo-sequence information (i.e., changing slope and/or terrain curvature with altitude) generated from geomorphometric analysis uniquely differentiates the lower portion of the Raikot Glacier surface from the surrounding landscape in the Raikot Basin at Nanga Parbat, Pakistan. Slope angles are relatively low over the glacier surface compared to those over non-glacier terrain at similar elevation. The topo-sequence information significantly constrains the location of the Raikot Glacier and does a good job delineating the ablation area. We are currently working on processing stages 4 and 5, although it is clear that the integration and use of additional image and topographic information will permit robust analysis and results.

3.2.4. Generation of DEMs from ASTER stereo

DEMs are needed for atmospheric correction of satellite imagery (Bishop et al., 2004; and this contribution), orthorectification (i.e., correction of panoramic distortion) of ASTER and other satellite images (Kääb 2002, 2004; Kääb et al., 2005), for deriving three-dimensional glacier parameters (Kääb et al., 2002; Paul et al., 2002; Paul, 2004; Khalsa et al., 2004), for assessing glacier thickness changes (Kääb, 2004), for multi-dimensional feature classification (e.g., of debris-covered ice; Paul et al., 2004a), and for other geomorphometric tasks (Bishop et al., 2004, and this contribution). The EDC in the USA generates DEMs from ASTER data on demand, but GLIMS has developed the same capability for greater flexibility and higher potential throughput.

Either level 1B data or level 1A data can be used for generation of DEMs from ASTER data. Level 1A data are the preferred source, because the geometry of level 1A imagery is known and therefore the stereo model can be precisely defined, but the data contain scan-line noise must be removed using the parameters provided by the image header. The geometry of level 1B imagery has been modified through projection onto a grid, and therefore the stereo model is created using an approximation such as a polynomial or rational function, introducing additional errors. For both level 1A and 1B data, orientation of the 3N and corresponding 3B band from ground control points (GCPs), transformation to epipolar geometry, parallax-matching, and

parallax-to-DEM conversion may be done using the PCI Geomatica Orthoengine software (Toutin and Cheng, 2001; Toutin, 2002) or other software packages, such as ENVI or ERDAS Imagine. GLIMS currently uses ENVI and PCI. Independently known elevations of GCPs corresponding to immobile points (such as major road intersections and unglacierized mountain peaks) are desirable for generation of the most accurate DEMs. In areas lacking sufficient GCPs, ground control may be computed directly from the known satellite position and rotation angles, although this yields less precise results. In such cases, the line of sight for an individual image point is intersected with the earth ellipsoid. The resulting position on the ellipsoid is corrected for the actual point elevation, which, in turn, is estimated from the band 3N–3B parallax of the selected GCP. Such GCPs can then be imported into PCI Geomatica for bundle adjustment. Further details on the above procedures can be found in Kääb (2002, 2004); Kääb et al. (2003).

The accuracy of ASTER DEMs was assessed through a number of test studies in which ASTER DEMs were compared to aerophotogrammetric reference DEMs and the SRTM DEM. The SRTM DEM represents, together with ASTER DEMs, one of the few globally available high-resolution DEMs and is thus of high importance to GLIMS. A first test site around Gruben Glacier in the Swiss Alps represents rugged high-mountain conditions with elevations of 1500–4000 m a.s.l., and includes a number of challenges to DEM generation, including steep rock walls, deep shadows, and snow fields lacking contrast (Kääb, 2004). Therefore, the test area is considered to represent a near-worst case for DEM generation from ASTER stereo data. Gries Glacier area, a second test site, represents less rugged high-mountain topography compared to the Gruben area. Nevertheless, the ASTER image used contains a greater number of low-contrast snow and ice areas (Kääb, 2004). A third test study was performed for the tongue of Glaciar Chico. Glaciar Chico is a northeastern outlet glacier of the Southern Patagonia Icefield partially calving into a branch of the Lago O' Higgins. The site represents moderate mountain topography including a large glacier with little optical contrast in the applied ASTER scene (Kääb, 2004). (For further tests of ASTER DEMs see also Toutin (2002); Hirano et al. (2003); Stevens et al. (2004).)

Visual inspection and quantitative analysis show that severe vertical errors of the ASTER DEMs of up to 500 m occur for sharp peaks having steep northern slopes (Fig. 6). These errors are not surprising, considering that northern slopes are heavily distorted (or even totally hidden) in the $27.6°$ back-looking band 3B, and lie in shadow as well for northern hemisphere sites. For the Gruben site, the accuracy obtained for the ASTER DEMs compared to the aerophotogrammetric reference DEM amounts to approximately ± 70 m RMS (Fig. 7). The vertical differences between the level 1A- and level 1B-derived DEMs amount to approximately ± 30 m RMS (range -380 to $+180$ m) (Fig. 7). For a subsection with moderate high-mountain topography, an accuracy of about ± 15 m RMS and maximum errors of 100 m were found (Kääb, 2004). These maximum errors occur at sharp moraine ridges or deep stream channels. Errors of that scale and even more are to be expected in densely forested areas just due to the height of tree canopy and due to mismatches from self-similar canopy features.

For the Gries Glacier test site, errors were significantly lower, and an RMS of ± 35 m was achieved (Fig. 7). Compared to the Gruben ASTER DEM, the Gries DEM reveals significantly fewer gross errors, but a lower accuracy for large terrain sections. This is most probably due to the lower optical contrast in the Gries area compared to the Gruben area at image acquisition time. For the Chico test site, the ASTER DEM turned out to show larger maximum errors compared to the Gruben site, but smaller maximum errors compared to the Gries test site (Fig. 7).

Errors of at least 10 m are possible on mountain peaks due to interannual and interseasonal variations of snow depth. Besides those factors, with a pixel resolution of 15 m in VNIR, vertical errors typically on the order of 15 m will be produced just due to unresolved topography in areas of steep and variable slopes. Thus, the typical DEM errors can be understood to be a result of real but transient variations in surface relief compounded by unresolved relief. The more extreme DEM errors or nulls clearly reveal other problems, such as terrain obscured by steep slopes, cloud interference, saturated pixels, pixels naturally lacking slope variations or topographic roughness, or residual errors in registration. In other DEM applications, lake surfaces routinely produce null points (with rare exceptions where sediment plumes or icebergs produce features that can yield parallax).

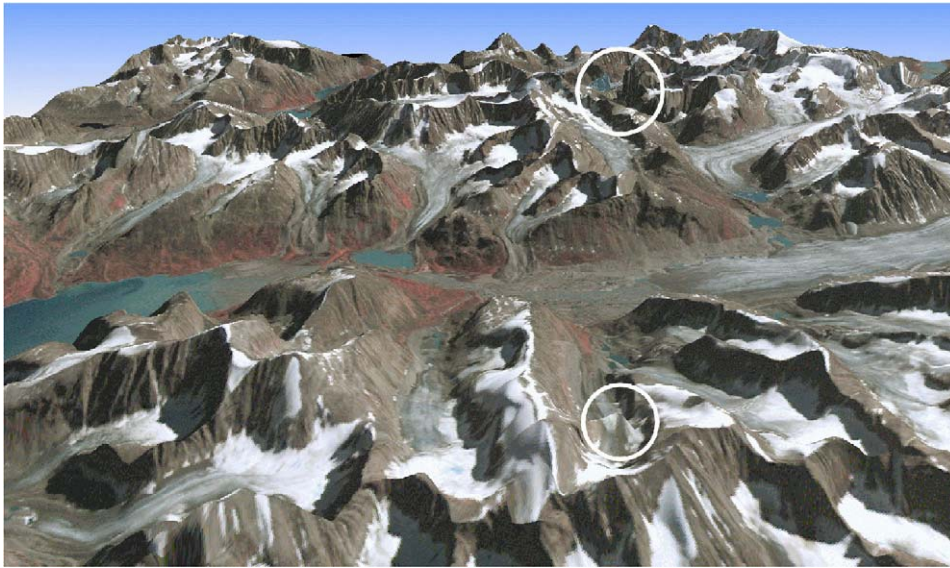Comparison between the SRTM3 DEM and the ASTER DEMs for the Gruben and Chico sites

Fig. 6. Synthetic perspective view of terrain on Baffin Island towards east with ASTER image draped over ASTER-derived DEM. Elevation outliers are marked by white circles.
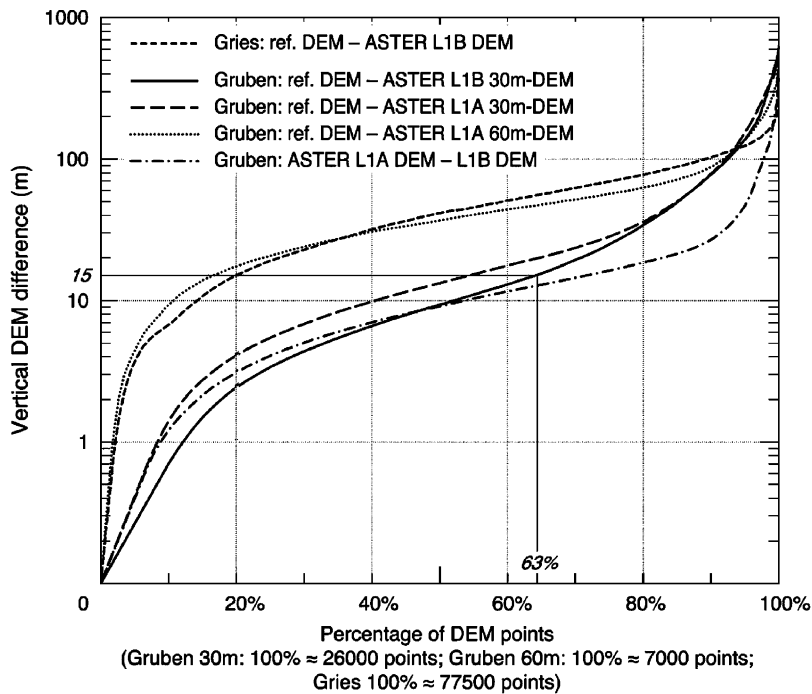

Fig. 7. Cumulative histogram of vertical deviations between aerophotogrammetric reference DEMs and ASTER level 1A- or level 1B-derived DEMs. For ASTER level 1B-derived DEM of Gruben area, for instance, 63% of points show a vertical deviation of ± 15 m RMS or smaller, i.e., ASTER pixel size in visible and VNIR (Kääb, 2004).

revealed that both DEMs are comparable for about 60% of the DEM points (Kääb, 2004) (Fig. 8). For the remaining points, the SRTM3 DEM shows significantly fewer severe errors. This effect is partly because the SRTM3 DEM shows more data gaps for difficult terrain conditions compared to the ASTER DEMs. In the SRTM3 such DEM sections are removed, whereas they are for the most part included in the ASTER DEMs investigated here. As a consequence,
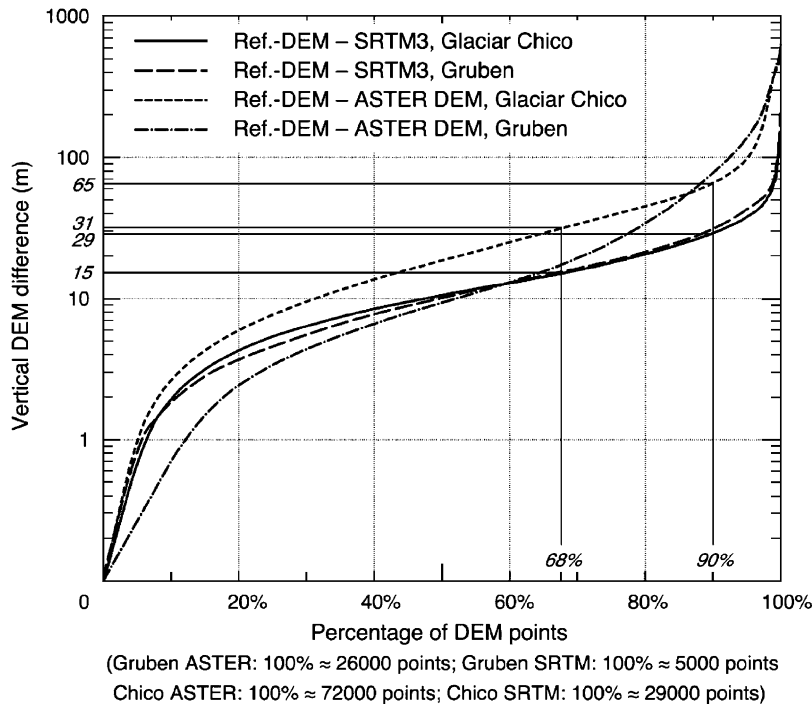
Fig. 8. Cumulative histograms of vertical deviations between aerophotogrammetric reference DEMs and ASTER or SRTM3 DEMs, respectively, for Glaciar Chico and Gruben. For Glaciar Chico, 68% of points have vertical deviations smaller than ±15 m for SRTM3 DEM, or smaller than ±31 m for ASTER DEM. For 90% level (LE90), corresponding numbers are ±29 m for SRTM3 and ±65 m for ASTER. (Kääb, 2004; Kääb, 2005).

ASTER DEMs can be used to fill SRTM3 DEM gaps and vice versa.

The tests presented above are based on ASTER DEMs derived using a grid spacing of 2 pixels (i.e., 30 m). While such resolution was found to improve the accuracy and representation of terrain details, coarser DEMs showed reduced severe errors. For vertical deviations smaller than about 100 m from the reference DEM (about 90% of the total point number), an ASTER DEM of the Gruben area derived with 60 m resolution gave larger deviations compared to the corresponding 30 m DEM. However, for the remaining 10% of DEM points with vertical deviations larger than 100 m, the 60 m DEM shows better vertical accuracy compared to the 30 m DEM (maximum error of 60 m DEM: 430 m). Accordingly, computation of multiple-resolution DEMs from one ASTER stereo data set and comparison of the results can be applied for detection and removal/masking of gross errors (Zollinger 2003; Kääb et al., 2005). The nulls generated by masking these errors then can be filled in with digitized paper topographic map data, SRTM DEMs, or can be interpolated from the ASTER DEM.

While the resolution of ASTER DEMs can make change detection of small glaciers difficult on the annual time scale, they can be used to good effect on larger and more rapidly changing glaciers, and their use in orthorectification of imagery leads to more accurate glacier outlines even for the smaller glaciers.

In summary, the availability of SRTM DEMs between 56°S and 60°N and the capability of generating DEMs from along-track ASTER stereo pairs enable GLIMS to orthorectify imagery over much of the glacierized terrain on Earth (excluding Greenland and Antarctica), and thereby produce high-accuracy glacier outlines for the GLIMS Glacier Database.

3.2.5. Glacier surface velocities

Horizontal displacements on glaciers have been measured using optical satellite imagery, mostly from repeated Landsat or SPOT data, using different correlation techniques (e.g., Lucchitta and Ferguson, 1986; Scambos et al., 1992; Skvarça et al., 2003). For such work, the spatial resolution of the applied imagery is, besides the time period between the acquisitions, the most crucial para-

meter. Unique surface features, usually crevasses or debris cover, must create trackable patterns in the imagery at the available resolution. Together with sensors of similar resolution (for instance SPOT pan, IRS pan, or Landsat7 ETM + pan), ASTER is well suited to this purpose with its 15 m VNIR resolution. Within GLIMS, glacier surface velocities represent a fundamental glacier parameter to be mapped and monitored (Raup et al., 2001; Kääb 2004; Kääb, 2005), but help also in assessing glacier hazards (Kääb 2002; Kääb 2005; this contribution).

Multi-temporal orthoimages obtained from repeated ASTER imagery are used to measure displacements of the glacier surface, and hence its velocity. In order to avoid distortions between the multi-temporal products, all imagery (i.e., 3N and 3B of time 1, and 3N and 3B of time 2) is adjusted as one image block connected by tie-points, before DEM generation and orthoprojection is performed (Kääb, 2002; Kääb, 2005). The tie-points for the multi-temporal model connection must be placed on stable terrain. The displacement of surface features between the multi-temporal satellite orthoimages is determined using image cross-correlation techniques (e.g., Scambos et al., 1992; Evans, 2000; Kääb, 2002). Matching errors are detected and eliminated based on insufficient correlation strength and by applying physical constraints, such as expected flow speed and direction, and limits on the strain rate of ice. In the case of coherent displacement fields, additional spatial filters may be applied such as vector median or RMS thresholds (Astola et al.,

1990; Kääb, 2004). Using the orthoimage georeference, the resulting displacement parallax field can be directly transformed into horizontal terrain displacements. Considering the sometimes vague definition of surface features and the terrain changes between the acquisition times, an overall accuracy of approximately 0.5–1 pixel size (i.e., 8–15 m for ASTER) can be expected for the horizontal displacement measurements (Kääb 2002, 2004).

The size of the image chips for image cross-correlation has to be chosen according to the textural characteristics of the imaged surface. If the reference chip size is too small, the correlation coefficients have no clear maximum; if the reference chip size is too large, computing time soars drastically, and the spatial resolution of the resulting displacement field is reduced. Typical reference chip sizes we apply to ASTER imagery for mountain glaciers range from 7×7 pixels to 15×15 pixels. Applications of repeated ASTER imagery for glacier velocity measurements are presented in Fig. 9, with further examples in Kääb (2002, 2004); Dowdeswell and Benham (2003); Kääb et al. (2004); Kääb (2005). A similar application using Landsat7 ETM + pan is presented by Skvarça et al. (2003).

The GLIMS Glacier Database is designed to be able to hold velocity field vectors on a per-glacier basis. While no velocity vector fields produced within the GLIMS project have yet been inserted into the database, several are in the queue, and we expect to incorporate the velocity vector sets from
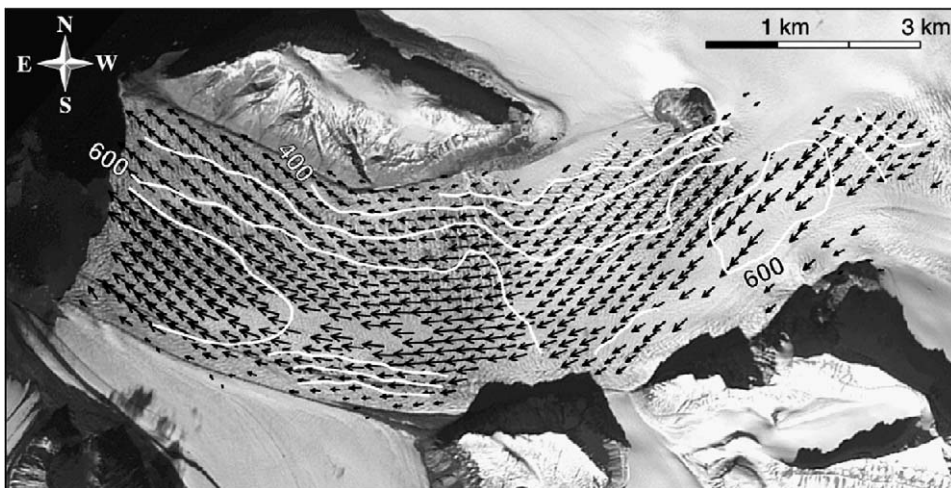

Fig. 9. Surface velocity field for a section of Kronebreen, Svalbard, derived from ASTER imagery of 26 June and 6 August 2001 (Kääb et al., 2004). Isolines indicate ice speed in meters per year. Surface velocities of Kongsvegen, joining Kronebreen to south of image section, are too small to be measured from repeated satellite imagery. Underlying ASTER image is from 6 August 2001.

the VELMAP Antarctic velocity data sets at http://nsidc.org/data/nsidc-0070.html.

3.2.6. Use of ASTER thermal imaging to aid interpretations

Thermal imaging of glaciers has proven useful in identifying various glacier facies (Taschner and Ranzi, 2002). Thermal methods may involve thermal inertia measurements if multiple looks at several times of day can be provided, material distinction due to differing thermal inertia and differential heating in morning looks, and observation of the thermal buffering by the latent heat of crystallization/melting of H_2O. The latter approach is used in a sample application here.

Because of the low (90 m) spatial resolution of ASTER's thermal bands compared to VNIR (15 m) and SWIR (30 m), and specifically due to pixel size being generally less than most glacier margin changes over periods of a few years, TIR bands or AST08 temperature images are of limited direct use for classification purposes. However, they can be a tremendous aid to scientific interpretation, including (1) delineation of melt-zone areas of glacier surfaces (thus indirectly aiding classification) and (2) identification of glacier areas that are thinly blanketed by rock debris and therefore look spectrally like morainal material. The temperature of supraglacial lakes can also be investigated using thermal emission data.

An example of glacier lake temperature mapping and interpretation is provided in Fig. 10. This figure shows some iceberg-cluttered lakes as having temperatures very close to the ice point; the 1–2 K-positive anomaly could be a calibration error (specified calibration error for ASTER's TIR subsystem is 1 K in the 270–340 K range (Thome 1998) and expected uncertainty in AST08 is between 1.5 and 3 K for this application) or could be due to thermal contamination from debris atop small icebergs; or perhaps the lake is warmer than the ice point and is actively melting the bergs. If we take the two iceberg-cluttered lakes in region A of Fig. 10 as calibration points, assuming a temperature of 0 °C there, then we must subtract about 2.4 K from the AST08 temperatures; we are left with an uncertainty around 1 K. Certainly more calibration points are needed to make such a calibration more robust. Whether glacier lakes are at the ice point or warmer than it (a question raised by Wessels et al. (2002) in their analysis of ASTER thermal data for Himalayan glaciers) is commonly critical to the

stability of these lakes, as a small amount of superheat can melt drainage conduits. Other lakes and ponds near the stagnant terminus of the debris-covered Martian River Glacier are variously cold and warm, indicating variations in the degree of thermal interaction between ice and lake water. As of April 2006, the GLIMS Glacier Database contains no data based solely on TIR data; however, we expect that to change in the future.

3.3. Quality control (QC)

A concern for users of the GLIMS Glacier Database is data quality and consistency. Standardization and uniformity of analysis results is achieved partly by the structure of the database itself, including a core set of parameters that are based directly on those adopted previously by WGMS (Haeberli, 1998). However, the collection of glacier data for any digital inventory poses yet another set of challenges that no amount of parameter definition and basic instruction and advice is likely to solve. Despite large gains in the degree of automation of glacier classification in satellite imagery, human judgment and subjectivity remain essential to the process. The GLIMS Analysis Comparison Experiments (GLACE) (below) and QC steps taken at data ingest time are designed to ensure high-quality data in the GLIMS Glacier Database.

GLIMS data are submitted to the NSIDC, where they are subjected to QC steps before being inserted into the GLIMS Glacier Database. All data are automatically checked for polygon closure, integrity of references (e.g., that all glacier outline segments are tied to other glacier information via GLIMS glacier IDs), segment order and circulation direction of polygons, and proper numeric range. Data are visualized on a map for inspection by the ingest operator (currently B. Raup). If a data set has anything wrong with it, the submitter is notified so that the data can be fixed before data ingest. Finally, after the data have been inserted into the database and become publicly viewable via the web interface, the submitter is notified and requested to view the data set and check it for accuracy.

To quantify the consistency of data provided by different Regional Centers and to identify possible pitfalls in analysis, the GLIMS project carried out a pair of comparative image analysis experiments in which all Regional Centers were invited to analyze the same group of glaciers in one image. The first
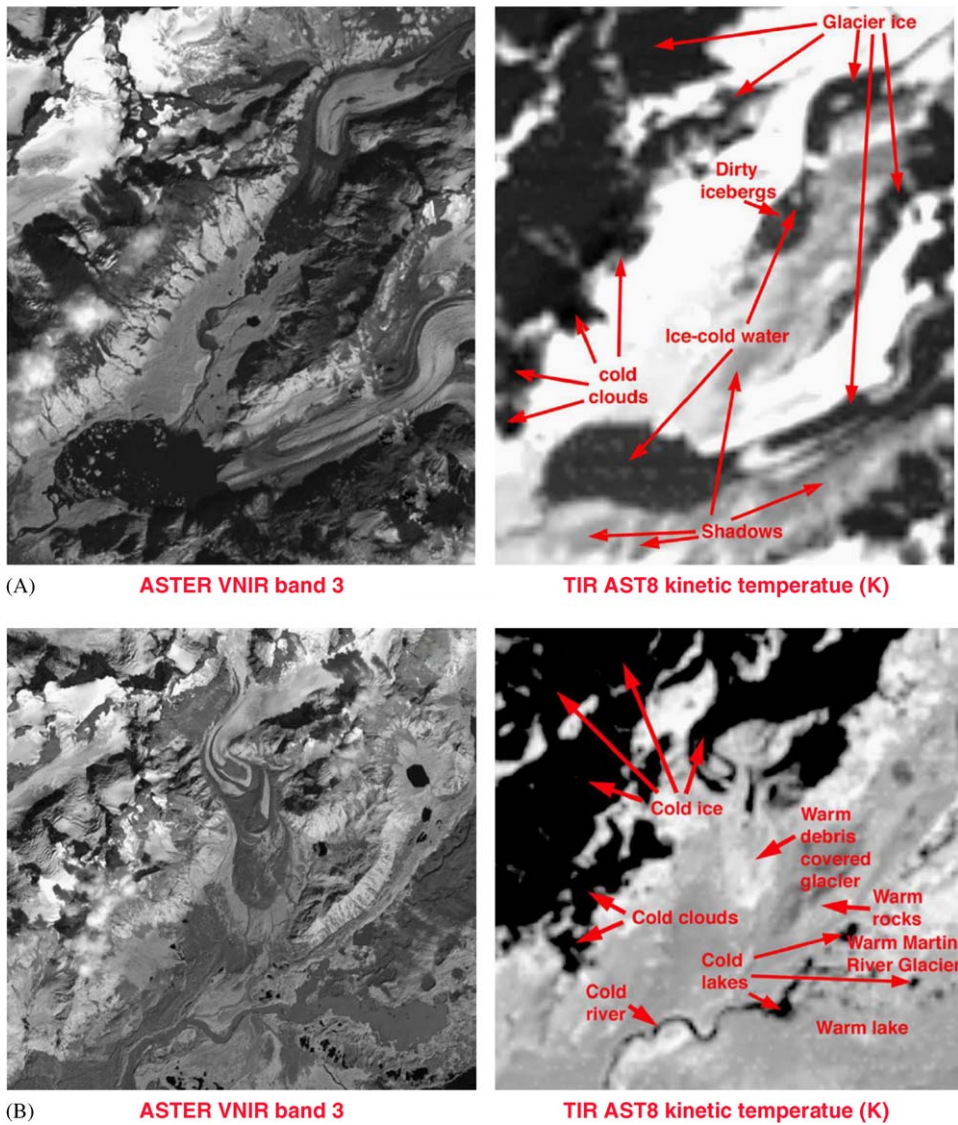
Fig. 10. Comparison of ASTER VNIR and thermal imaging of glaciers east of Copper River, Chugach Range, Alaska.

such experiment, originally called the Round-robin experiment, but now dubbed GLACE 1 was conducted in 2004 and results were reported at the August 2004 GLIMS Workshop in Oslo, Norway; the Fall 2004 meeting of the American Geophysical Union (Raup et al., 2004), and the December 2004 GLIMS Mini-workshop in San Francisco. Another such experiment (GLACE 2) was carried out in the autumn of 2005, and results were reported at the GLIMS Meeting in New Zealand in February 2006 and at the Arctic Workshop in Boulder, CO, in March 2006. Future comparisons may be further designed for use as a mandatory training exercise

across the GLIMS project. GLACE 2 emphasized change detection using multi-temporal optical imagery.

In GLACE 1, an ASTER image was chosen that contained a variety of glaciers, as well as several glacier boundary types: ice–water, ice–rock, snow–rock, snow divides. The analysis results, in the form of glacier outlines, were compiled, compared, and analyzed for consistency. Detailed results of both GLACE 1 and GLACE 2 will be published separately. In summary, the results were variable and included problems such as (1) geolocation errors, (2) interpretation errors, (3) interpretation

differences, and (4) algorithmic deficiencies. An example of an interpretation error is including non-glacier material, such as a rock slope or proglacial lake, within the glacier boundary. Interpretation differences result from varying definitions of what to include as glacier (Should the laterally adjacent snow slope be part of the glacier? Where does a debris-covered glacier end and partly ice-cored moraine that is separate from the glacier begin?). Algorithmic deficiencies led to the underestimation of glacier area in several cases. For example, parts of the tongues of some glaciers were lightly debris covered, leading some algorithms to mis-classify those regions as rock (non-glacier). The results with gross errors were useful in identifying pitfalls in the analysis process and point out the need for tighter protocols and standards. (Real data submissions with these kinds of errors do not pass the QC steps described above and are not ingested; the submitter is notified of the errors.) By reviewing these results, Regional Centers are able to improve their processing flow to avoid these errors. GLACE results that would have been deemed acceptable for ingest (passing basic QC steps described above) show good consistency, deviating from each other by only a few pixels in most places.

The problems encountered in GLACE 1 were largely mitigated in GLACE 2. However, interpretation differences remained, leading to an extensive discussion at the New Zealand GLIMS Meeting, and since then on the GLIMS mailing list, about how to specify a strict practical definition of the term "glacier" for use within the GLIMS project. An additional feature of the GLACE 2 experiment was analysis of two images, separate by 9 years, of the same glacier system. Participating Regional Centers produced a set of glacier outlines from each image and provided an estimate of area change for the glacier. Some analyses showed a slight increase in area, while others showed a slight decrease. The overall result showed area change that was not statistically different from zero.

As a consequence of the GLACE experiments, GLIMS is developing a series of guidelines, definitions, standard protocols, and standard analysis modules that Regional Centers will use in order to produce uniform glacier data for GLIMS. These standard analysis modules are being implemented in GLIMSView, and a data submission website has been created that captures metadata on processing steps used. A major new release of GLIMSView is expected in summer 2006 that will introduce a suite of standard tools that will satisfy some, though not all, of the need for standardized analysis. Once these tools are implemented and guidelines are set out, we anticipate conducting more comparative image analysis experiments to validate the protocols and analysis modules as they evolve. GLIMSView will be the chief vehicle for ensuring adherence to standardization protocols by guiding the analyst through predetermined processing steps in the protocol, or through its use as a "filter" program, which will ensure that certain processing steps have been taken before exporting the data into the data transfer format. We do not expect use of GLIMS-View to be a hindrance, but rather to be a great facilitator of analysis by virtue of its ease of use and reliability of derived data (and distribution at no cost to the user).

The GLACE experiments have shown mixed results, but are propelling the creation and adoption of standard definitions and processing procedures. The final QC stage is highly important, and has resulted in much higher consistency of data currently in the GLIMS Glacier Database than was exhibited in the GLACE tests.

4. Results

4.1. GLIMS glacier database

The design of a geospatial database for storing information about glaciers presents some particular challenges. The GLIMS database (Raup et al., 2001, http://www.glims.org/MapsAndDocs/db_design. html) must represent time-varying information about a set of objects, which in some cases have tree-like relationships between them. The analyses producing this information are performed using a variety of input sources (imagery from various satellites, air photos, and maps) and methods including both automatic algorithms and manual interpretation. As described above, a standard protocol is being developed and implemented in GLIMSView, but a considerable amount of manual editing and human choice of automatic processing tools—hence, subjective interpretation—will remain in the processing stream for some time, and hence will affect the resulting data. GLIMS glacier data come from many researchers from around the world. A wealth of metadata about the analysis and even a little about the analyst must be accommodated. The results of glacier analysis at

the various Regional Centers are sent to NSIDC in Boulder, CO, USA.

The GLIMS Glacier Database is implemented as a geospatial relational database. The two main tables are called Glacier_Static and Glacier_Dynamic. The first stores static (normally unchanging) information, such as the glacier's name and location. The second stores all of the measured attributes of a glacier that are associated with a specific time, e.g., its outline, a vector delineating the transient snow line, WGMS glacier classification parameters, and speed. Other tables store related information such as image and map metadata, browse and other raster data, glacier hypsometric data, and information about GLIMS institutions and data contributors. The Glacier_Dynamic table carries a time stamp identifying the time represented by the information. As a result, the database can store a time series of glacier data that can be analyzed for trends, and is thus a good tool for detection of changes in Earth's cryosphere and climate.

Glaciers are identified in the database using an ID composed from its longitude and latitude, such as "G225691E58672N" (i.e., 58.672°N and 225.691°E) for the Taku Glacier in Alaska. With this scheme, analysts can assign IDs without fear of their assignments colliding with those of other analysts.

As a glacier retreats, it can separate into two or more parts. In order to keep track of the relationship between these smaller remnants and the larger glacier from which they formed, the Glacier_Static table contains a field that can store the ID of a glacier's parent ice mass. A remnant would be given a new glacier ID, and the ID of its parent is stored. This scheme for representing parent–child relationships between records in the database is also useful in the case when a large ice mass is initially analyzed and entered into the database as one glacier, and then it is subsequently analyzed in more detail, where different parts of it are identified as glaciers in their own right and given their own glacier IDs. Using the "parent ice mass" field, the continuity of analyses stretching over time and levels of detail is preserved, such that an analyst can later repeat the original analysis or update it, and thus validate the earlier work or produce a time series using the same glacier definitions.

The database is designed to be a logical extension of the WGI of WGMS. Each snapshot of a glacier in the Glacier_Dynamic table can store the full complement of WGMS-defined glacier characteristics used in the WGI, including parameters such as primary glacier classification, glacier form, and dominant mass source. The GLIMS Glacier Database therefore is extending the WGI by adding multiple snapshots over time, by increasing the number of glaciers covered, and by storing full glacier outlines, rather than just point locations.

NSIDC has implemented the GLIMS Glacier Database using the Open Source relational database engine PostgreSQL, which has been augmented with geospatial data types and functionality provided by PostGIS. NSIDC has also created a map-based worldwide web interface to the database (http://glims.colorado.edu/glacierdata/). The Open Source package MapServer connects directly to the database and presents interactive maps of the data (Fig. 11). Layers available to the user include glacier outlines, footprints of ASTER imagery acquired over glaciers, the WGI, Regional Center areas of interest, GLIMS collaborators, glacier area from the Digital Chart of the World, and other supporting layers such as country borders. The user can search for subsets of glacier data, applying constraints such as time range, geographic area, glacier classification, and the results are presented in a map image, together with selected attribute data. The results of such a query may then be downloaded to the user's computer in a choice of GIS formats, including ESRI Shapefiles and the multi-segment ASCII format of Generic Mapping Tools (Wessel and Smith, 1998, http://gmt.soest.hawaii.edu/). The server can function as an Open Geospatial Consortium-compliant Web Map Service, serving map layers to other web map servers. NSIDC is also implementing a web coverage service, which provides raster data to other servers, and a web feature service, which provides vector data in a machine-readable format.

As of April 2006, the GLIMS Glacier Database contains "snapshots" of approximately 52 000 glaciers, with more data expected soon from several Regional Centers. Each snapshot consists of, at minimum, a glacier outline and information about who produced the data, by what methods, and a timestamp for when the outline applies. Many records contain additional information, including snow line or center-line locations, or outlines for debris cover, supraglacial lakes, or proglacial lakes. Fig. 12 shows a map of GLIMS glacier outlines (red) and, for reference, WGI data (blue). At this scale, the size of glaciers is exaggerated to make
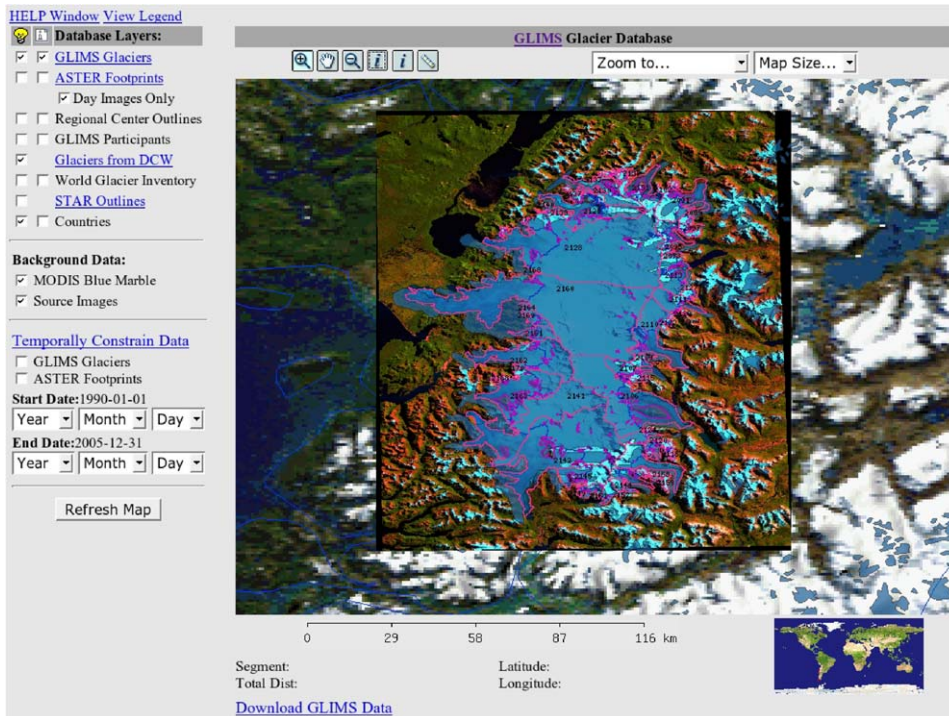
Fig. 11. Depiction of a typical view of web-based interface to GLIMS Glacier Database in a web browser. Background image, MODIS "blue marble" mosaic; higher-resolution inset image, Landsat 5 mosaic; translucent blue shading, glacier layer from Digital Chart of World; red lines, GLIMS glacier outlines; blue lines, glacier snow lines (inside Landsat image) or country borders (outside Landsat image).
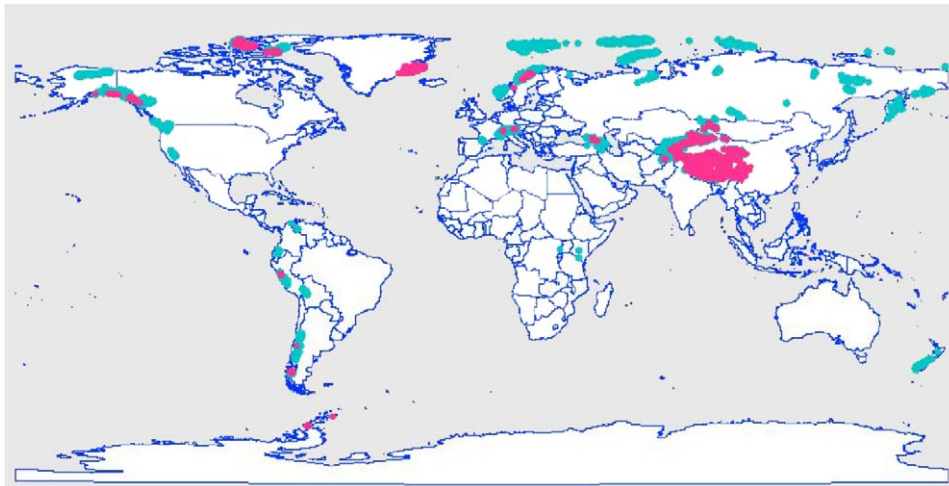

Fig. 12. Map of glacier "snapshots" in GLIMS Glacier Database as of April 2006 (red) and WGI Glacier locations plotted as points (blue) for reference.

them more visible. Data production is accelerating, and we expect data for several more regions, including New Zealand, European Alps, and Alaska, in the coming two years.

5. Discussion and conclusions

GLIMS is composed of many institutions with varying technical expertise, deriving from satellite

imagery information about glaciers that have widely varying characteristics. This necessitates special care in standardizing the production of glacier data, in transferring the data to the data archive center (NSIDC), in designing the database to represent all of the many types of glaciers and their inter-relationships, and in designing an interface to present this complex data set to the world. GLIMS has addressed these obstacles by developing standard protocols for image classification and glacier analysis, by developing software to implement these protocols, and by designing a database and a web interface that represent the complexity of Earth's glacier systems.

For the first time in glaciological history, a global digital inventory of glaciers, together with their outlines, is under way. A number of disciplines will be able to profit from the GLIMS Glacier Database, e.g., climate modeling, climate change research, hydrology and water resource management, and hazard monitoring and mitigation. In the coming years, repeated inventorying will allow studies of glacier change and the pace of change. The ASTER instrument is expected to operate through 2009, but future GLIMS work will be done using other sensors as they become operational, possibly including the French Satellites d'Observation de la Terre, the Japanese Advanced Land Observing Satellite, and follow-ons to the EO-1 experimental satellite, as well as radar instruments. We also plan to implement multi-scale approaches to glacier mapping, using coarser spatial resolution instruments such as MODIS to build a first-order map of glacier extent. There has never been a greater need for global and rapid remote sensing-based glacier mapping, and GLIMS hopes to provide such data to the broader scientific communities.

Acknowledgments

References

Abdalati, W., Steffen, K., 2001. Greenland ice sheet melt extent: 1979–1999. Journal of Geophysical Research 106, 33983–33988.

Abdalati, W., Krabill, W., Frederick, E., Manizade, S., Martin, C., Sonntag, J., Swift, R., Thomas, R., Wright, W., Yungel, J., 2001. Outlet glacier and margin elevation changes: near-coastal thinning of the Greenland ice sheet. Journal of Geophysical Research 106, 33729–33741.

Abdalati, W., Krabill, W., Frederick, E., Manizade, S., Martin, C., Sonntag, J., Swift, R., Thomas, R., Yungel, J., 2004. Elevation changes of ice caps in the Canadian Arctic Archipelago. Journal of Geophysical Research 109, F04007.

Albert, T.H., 2002. Evaluation of remote sensing techniques for ice-area classification applied to the tropical Quelccaya ice cap, Peru. Polar Geography 26, 210–226.

Astola, J., Petri, H., Yrjo, N., 1990. Vector median filters. Proceedings of the IEEE 78, 678–689.

Baltsavias, E.P., Favey, E., Bauder, A., Boesch, H., Pateraki, M., 2001. Digital surface modelling by airborne laser scanning and digital photogrammetry for glacier monitoring. Photogrammetric Record 17, 243–273.

Bamber, J.L., Vaughan, D.G., Joughin, I., 2000. Widespread complex flow in the interior of the Antarctic ice sheet. Science 287:1248.

Bayr, I.J., Hall, D.K., Kovalick, W.M., 1994. Observations on glaciers in the eastern Austrian Alps using satellite data. International Journal of Remote Sensing 15, 1733–1742.

Bishop, M.P., Bonk, R., Kamp Jr., U., Shroder Jr., J.F., 2001. Terrain analysis and data modeling for alpine glacier mapping. Polar Geography 25, 182–201.

Bishop, M.P., Olsenholler, J.A., Shroder, J.F., Barry, R.B., Raup, B.H., Bush, A.B.G., Copland, L., Dwyer, J.L., Fountain, A.G., Haeberli, W., Kääb, A., Paul, F., Hall, D.K., Kargel, J.S., Molnia, B.F., Trabant, D.C., Wessels, R., 2004. Global land Ice measurements from space (GLIMS): remote sensing and GIS investigations of the Earth's cryosphere. Geocarto International 19, 57–89.

Church, J.A., et al., 2001. In: Houghton, J.T., et al. (Eds.), Climate Change 2001: The Scientific Basis. Cambridge University Press, Cambridge, pp. 639–693.

Dowdeswell, J.A., Benham, T.J., 2003. A surge of Perseibreen, Svalbard, examined using aerial photography and ASTER high-resolution satellite imagery. Polar Research 22, 373–383.

Dyurgerov, M.B., Bahr, D.B., 1999. Correlations between glacier properties: finding appropriate parameters for global glacier monitoring. Journal of Glaciology 45, 9–16.

Dyurgerov, M.B., Meier, M.F., 2000. Twentieth century climate change: evidence from small glaciers. Proceedings of the National Academy of Sciences 97, 1406–1411.

Evans, A.N., 2000. Glacier surface motion computation from digital image sequences. IEEE Transactions on Geoscience and Remote Sensing 38, 1064–1072.

Gao, J., Liu, Y., 2001. Applications of remote sensing, GIS and GPS in glaciology: a review. Progress in Physical Geography 25, 520–540.

Geist, T., Stötter, J., 2003. First results of airborne laser scanning technology as a tool for the quantification of glacier mass balance, In: EARSEL eProceedings, LISSIG Workshop, 11–13 March 2002, Berne, vol. 2, pp. 8–14.

Gregory, J.M., Oerlemans, J., 1998. Simulated future sea-level rise due to glacier melt based on regionally and seasonally resolved temperature changes. Nature 391, 474–476.

Haeberli, W., 1998. Historical evolution and operational aspects of worldwide glacier monitoring. In: Haeberli, W., Hoelzle, M., Suter, S. (Eds.), Into the Second Century of World Glacier Monitoring—Prospects and Strategies. UNESCO Publishing, Paris, pp. 35–51.

Haeberli, W., Beniston, M., 1998. Climate change and its impacts on glaciers and permafrost in the Alps. Ambio 27, 258–265.

Hastenrath, S., Geischar, L., 1997. Glacier recession on Kilimanjaro, East Africa, 1912–1989. Journal of Glaciology 43, 455–459.

Hirano, A., Welch, R., Lang, H., 2003. Mapping from ASTER stereo image data: DEM validation and accuracy assessment. Photogrammetry and Remote Sensing 57, 356–370.

Huggel, C., Kääb, A., Haeberli, W., Teysseire, P., Paul, F., 2002. Remote sensing based assessment of hazards from glacier lake outbursts: a case study in the Swiss Alps. Canadian Geotechnical Journal 39, 316–330.

Joughin, I., 2002. Ice-sheet velocity mapping: a combined interferometric and speckle-tracking approach. Annals of Glaciology 34, 195–201.

Joughin, I., Tulaczyk, S., Bindschadler, R., Price, S.F., 2002. Changes in west Antarctic ice stream velocities: observation and analysis. Journal of Geophysical Research 107, B1/2289.

Kääb, A., 2002. Monitoring high-mountain terrain deformation from repeated air- and spaceborne optical data: examples using digital aerial imagery and ASTER data. Photogrammetry and Remote Sensing 57, 39–52.

Kääb, A., 2004. Mountain glaciers and permafrost creep. Methodical research perspectives from Earth observation and geoinformatics technoligies. Habilitation Thesis, Department of Geography, University of Zurich, 205 pp.

Kääb, A., Paul, F., Maisch, M., Hoelzle, M., Haeberli, W., 2002. The new remote-sensing-derived Swiss glacier inventory: II. First results. Annals of Glaciology 34, 362–366.

Kääb, A., Huggel, C., Paul, F., Wessels, R., Raup, B., Kieffer, H., Kargel, J., 2003. Glacier monitoring from ASTER imagery: accuracy and applications. In: EARSEL eProceedings, LISSIG Workshop, 11–13 March 2002, Berne, vol. 2, pp. 43–53.

Kääb, A., Reynolds, J.M., Haeberli, W., 2005. Glacier and permafrost hazards in high mountains. In: Huber, U.M., Bugmann, H.K.M., Reasoner, M.A. (Eds.), Global Change and Mountain Regions: An Overview of Current Knowledge. Springer, Berlin, pp. 225–234.

Kargel, J.S., et al., 2005. Multispectral imaging contributions to global land ice measurements from space. Remote Sensing of Environment 99, 187–219.

Khalsa, S.J.S., Dyurgerov, M.B., Khromova, T., Raup, B.H., Barry, R.G., 2004. Space-based mapping of glacier changes using ASTER and GIS tools. IEEE Transactions on Geoscience and Remote Sensing 42, 2177–2182.

Kieffer, H., et al., 2000. New eyes in the sky measure glaciers and ice sheets. EOS Transactions, American Geophysical Union 81, 265, 270, 271.

Krabill, F., Frederick, E., Manizade, S., Martin, C., Sonntag, J., Swift, R., Thomas, R., Wright, W., Yungel, J., 1999. Rapid thinning of parts of the southern Greenland ice sheet. Science 283, 1522–1524.

Krabill, W., Hanna, E., Huybrechts, P., Abdalati, W., Cappelen, J., Csatho, B., Frederick, E., Manizade, S., Martin, C., Sonntag, J., Swift, R., Thomas, R., Yungel, J., 2004. Greenland ice sheet: increased coastal thinning. Geophysical Research Letters 31 (24), 1–4.

Lucchitta, B.K., Ferguson, H.M., 1986. Antarctica: measuring glacier velocity from satellite images. Science 234, 1105–1108.

Oerlemans, J., 2005. Extracting a climate signal from 169 glacier records. Science 308, 675–677.

Paterson, W.S.B., 1994. The Physics of Glaciers. Pergamon Press, Oxford.

Paul, F., 2002. Changes in glacier area in Tyrol, Austria, between 1969 and 1992 derived from Landsat 5 Thematic Mapper and Austrian glacier inventory data. International Journal of Remote Sensing 23, 787–799.

Paul, F., 2004. The new Swiss glacier inventory 2000—application of remote sensing and GIS. Ph.D. Thesis, Department of Geography, University of Zurich, 198 pp.

Paul, F., Kääb, A., in press. Challenges for glacier inventorying from multispectral satellite data in the Canadian Arctic: Cumberland Peninsula, Baffin Island. Annals of Glaciology 42.

Paul, F., Kääb, A., Maisch, M., Kellenberger, T., Haeberli, W., 2002. The new remote-sensing-derived Swiss glacier inventory: I. Methods. Annals of Glaciology 34, 355–361.

Paul, F., Huggel, C., Kääb, A., and Kellenberger, T., 2003. Comparison of TM-derived glacier areas with higher resolution data sets. In: EARSeL eProceedings of the EARSeL Workshop on Remote Sensing of Land Ice and Snow, 11–13 March 2002, Berne, vol. 2, pp. 15–21.

Paul, F., Kääb, A., Maisch, M., Kellenberger, T., Haeberli, W., 2004a. Combining satellite multispectral image data and a digital elevation model for mapping of debris-covered glaciers. Remote Sensing of Environment 89, 510–518.

Paul, F., Kääb, A., Maisch, M., Kellenberger, T., Haeberli, W., 2004b. Rapid disintegration of Alpine glaciers observed with satellite data. Geophysical Research Letters 31, L21402.

Raup, B.H., Kieffer, H.H., Hare, T.M., Kargel, J.S., 2000. Generation of data acquisition requests for the ASTER satellite instrument for monitoring a globally distributed target: glaciers. IEEE Transactions on Geoscience and Remote Sensing 38, 1105–1112.

Raup, B., Scharfen, G., Khalsa, S., Kaeaeb, A., 2001. The design of the GLIMS (Global Land Ice Measurements from Space) glacier database. EOS Transactions Suppl. 82, F542.

Raup, B., Khalsa, S.J.S., Armstrong, R., Cawkwell, F., Georges, C., Hamilton, G., Sneed Jr., W., Wheate, R., 2004. Comparative image analysis to ensure data quality in the global land ice measurements from space (GLIMS) glacier database. EOS Transactions supplement 85, 47 (Abstract H23D-1151).

Rignot, E., Casassa, G., Gogineni, P., Krabill, W., Rivera, A., Thomas, R., 2004a. Accelerated ice discharge from the Antarctic peninsula following the collapse of Larsen B ice shelf. Geophysical Research Letters 31, L18401.

Rignot, E., Braaten, D., Gogineni, S.P., Krabill, W., McConnell, J.R., 2004b. Rapid ice discharge from southeast Greenland glaciers. Geophysical Research Letters 31, L10401.

Rumelhart, D.E., McClelland, J.L., 1986. Parallel Distributed Processing: Exploration in the Microstructure of Cognition. MIT Press, Cambridge, MA.

Scambos, T.A., Dutkiewicz, M.J., Wilson, J.C., Bindschadler, R.A., 1992. Application of image cross-correlation to the measurement of glacier velocity using satellite image data. Remote Sensing of Environment 42, 177–186.

Sidjak, R.W., Wheate, R.D., 1999. Glacier mapping of the Illecillewaet icefield, British Columbia, Canada, using Landsat TM and digital elevation data. International Journal of Remote Sensing 20, 273–284.

Skvarça, P., Raup, B., De Angelis, H., 2003. Recent behaviour of Glaciar Upsala, a fast flowing calving glacier in Lago Argentino, Southern Patagonia. Annals of Glaciology 36, 184–188.

Stevens, N.F., Garbeil, H., Mouginis-Mark, P.J., 2004. NASA EOS Terra ASTER: volcanic topographic mapping and capability. Remote Sensing of Environment 90, 405–414.

Strozzi, T., Luckman, A., Murray, T., Wegmüller, U., Werner, C.L., 2002. Glacier motion estimation using SAR offset-tracking procedures. IEEE Transactions on Geoscience and Remote Sensing 40, 2384–2391.

Taschner, S., Ranzi, R., 2002. Comparing the opportunities of LANDSAT-TM and ASTER data for monitoring a debris covered glacier in the Italian alps within the GLIMS project.

In: Proceedings of the IGARSS 2002, Toronto, ISBN 0-7803-7537-8, pp. 1044–1046.

Thome, K., et al., 1998. ASTER preflight and inflight calibration and the validation of level 2 products. IEEE Transactions on Geoscience and Remote Sensing 36, 1161–1172.

Toutin, T., 2002. DEM from stereo Landsat 7 ETM + data over high relief areas. International Journal of Remote Sensing 23, 2133–2139.

Toutin, T., Cheng, P., 2001. DEM generation with ASTER stereo data. Earth Observation Magazine 10, 10–13.

Wessel, P., Smith, W.H.F., 1998. New, improved version of Generic Mapping Tools released. EOS Transactions, American Geophysical Union 79, 579.

Wessels, R.L., Kargel, J.S., Kieffer, H.H., 2002. ASTER measurement of supraglacial lakes in the Mount Everest region of the Himalaya. Annals of Glaciology 34, 399–408.

Williams, Jr., R.S., Ferrigno, J.G., 2002. Satellite image atlas of glaciers of the world: North America. US Geological Survey Professional Paper no. 1386-J.

Yang, Z., Hu, X., 1992. Study of glacier meltwater resources in China. Annals of Glaciology 16, 141–145.

Zollinger, S., 2003. ASTER satellite data for automatic generation of DEMs in high mountains. Diploma Thesis, Department of Geography, University of Zurich, Zurich.

Zwally, H.J., Abdalati, W., Herring, T., Larson, K., Saba, J., Steffen, K., 2002. Surface melt-induced acceleration of Greenland ice-sheet flow. Science 297, 218–222.